Compact 3-D Multilayer Substrate Integrated Circular and Elliptic Cavities (SICCs and SIECs) Dual-mode Filter with High Selectivity

Z. -G. Zhang, Y. Fan, and Y. -H. Zhang

Fundamental Science on Extreme High Frequency Key Laboratory
University of Electronic Science and Technology of China, Chengdu 611731, China
freemanzg@yahoo.com.cn, fanyong@ee.uestc.edu.cn, yhzhang@ee.uestc.edu.cn

Abstract ─ In this paper a multilayer dual-mode complementary filter is developed based on the substrate integrated circular and elliptic cavity (SICC and SIEC). The filter is constructed with a SICC and double SIECs, and each cavity supports two degenerate modes, which can be generated and controlled by the coupling aperture and the slot located between layers. With multilayer topology, the structures can exhibit vertical coupling between vertically stacked dual-mode cavities. It does not only have the good performance, but also reduces the circuit size much more. Moreover, sharp transition characteristic in both the lower side and the upper side demonstrates high selectivity of the filter. Good agreement is obtained between the simulated and measured results of the proposed structure.

Index Terms ─ Dual-mode filter, elliptic cavity, high selectivity, multilayer, substrate integrated circular cavity (SICC), and transmission zeros (TZs).

I. INTRODUCTION

Compact RF/microwave filters with high performance are key components, which are finding increasing application in modern wireless communication systems. Recently, substrate integrated waveguides (SIW) have been proposed [1-6], and applied to develop many high-quality components. Furthermore, the SIW provides a promising solution to low cost, low profile, and low weight, while high performance is maintained. Usually, SIW filters are made from rectangular cavities [1-3]. In [1], cross-coupling was provided by higher order modes in cavities. Due to the transmission zeros are far away from the passband, steep transition band was hard to realize. A compact SIW filter with defected ground structure (DGS) was proposed in [2]. However, the substrate integrated circular cavity (SICC) and elliptic cavity (SIEC) are both good choices in the design of high performance filter [4-9]. They not only have the same attractiveness as classical SIW filters [10, 11], but also present a higher quality factor and lower loss. In [4], a new topology of coupling between SICCs was designed to produce particular filtering functions. In [8], a planar diplexer was developed based on the dual-mode SICCs. However, the SIW technology faces a new problem about the circuit size. Recently, the dual-mode technology [8, 9, 12] has been introduced in the design of SIW filter to meet the requirements in size reduction. The dual-mode concept consists of using a pair of resonant modes within a single physical cavity, which not only reduces the circuit size more than half but also adds the design flexibility. On the other hand, the multilayer technology has become important, and is also another efficient way to achieve a compact circuit. In a 3-D multilayer substrate, more SIW circuits can be synthesized and accommodated into different layers and the coupling among them can easily be implemented to construct novel functional and compact structures. Therefore, the dual-mode and multilayer techniques can be combined together to achieve more compact SIW circuits. In [5], a fourth-order multilayer cross-coupled circular cavity filter was proposed. A Ka-band band pass filter has been proposed in [9] using dual-mode SICCs. A coupling via placed in the cavities was used to perturb the two degenerate modes. But, the via located in SICCs also

Submitted On: April 10, 2012
Accepted On: Nov. 25, 2012

decreased the quality factor of cavities, and the four layers circuit demonstrated an insertion loss of 2.95 dB and the stop-band rejection is below 25 dB. To achieve higher selectivity, an additional dual-mode SICC can be introduced in the above structure without increasing the circuit size. However, the lower sideband rejection can not be increased significantly because a SICC contributes only to the two transmission zeros (TZs) located at the upper side band. Interestingly, a SIEC exhibits quite different characteristic compared with a SICC. TZs are located in the lower side response of the elliptic cavity. Therefore, the SICC and SIEC techniques can be employed together to achieve multilayer complementary filter with higher performance.

In this paper, dual mode SICC and double SIECs are introduced in the 3-D multilayer SIW circuits and a compact dual-mode complementary filter with low loss, elliptic response and high selectivity have been achieved. The orientations of coupling aperture and slot relative to the major axis of the SIEC can be adjusted to generate two degenerate modes. Meanwhile, it is possible to control the bandwidth and the rejection level by adjusting parameters of the arc-shaped slot. The proposed structure is not only very compact, but has lower insertion loss, high selectivity and better stop-band rejection (> 50 dB). Moreover, it can be found that both the upper and the lower side response of the filter are very steep.

II. FILTER ANALYSIS AND DESIGN

A. Multilayer dual-mode complementary filter

As shown in Fig. 1, a SICC and double SIECs with three layers have been introduced to improve the performance of the filter. The first and last layers are used for input/output port. Three dual mode cavity resonators are coupled through arc-shaped coupling slots in metal layer 2 or layer 3. In these figures, W_C and W_S are the width of the coupling aperture and slot, respectively, θ is the central angle of the coupling slot, R_a and R_b are the semi-major and semi-minor axis of SIEC, respectively. While the symbol W_g is the width of the input and output SIWs. The symbol R is the radius of the SICC.

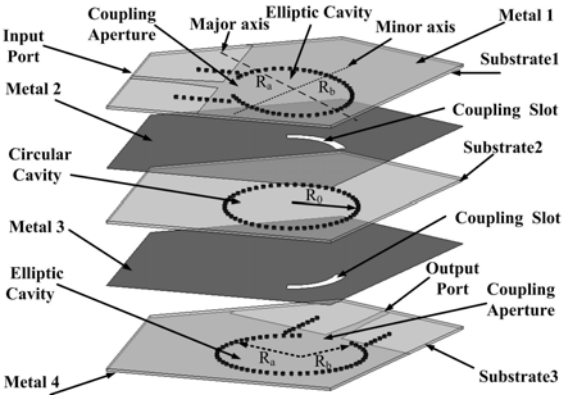

(a) Anatomy view

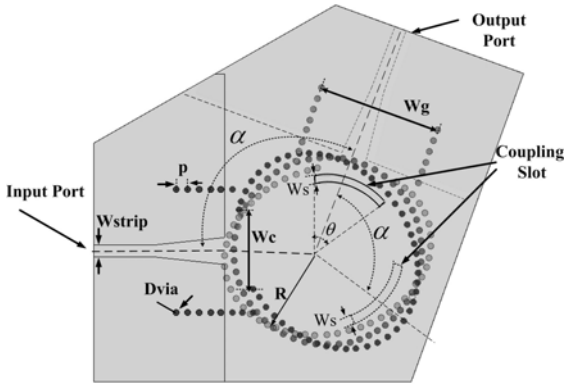

(b) Top view

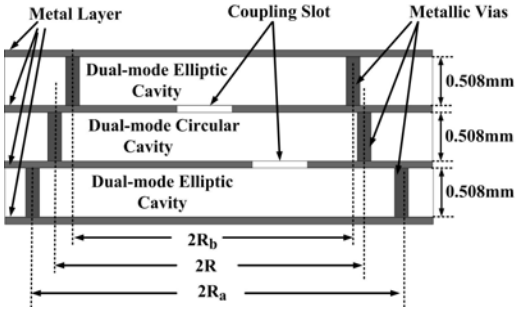

(c) Side view

Fig. 1. Proposed dual-mode SICC and SIEC filter with three layers.

B. Dual-mode SICC and SIEC principle

It is well known that the dual-mode phenomenon exists in a SICC and SIEC. Compared with the traditional rectangular cavity, the SICC and SIEC both are more suitable to be used as dual-mode cavities due to smooth inner surfaces. In a SICC, the degenerate modes are the horizontal and vertical TM_{110} mode. The resonant frequency for the

circular cavity with solid wall can be calculated using [13]

$$f_{mnp}=\begin{cases}\dfrac{c}{2\pi\sqrt{\mu_r\varepsilon_r}}\sqrt{\left(\dfrac{\mu'_{mn}}{R}\right)^2+\left(\dfrac{p\pi}{\Delta h}\right)^2} & TE_{mnp}\\ \dfrac{c}{2\pi\sqrt{\mu_r\varepsilon_r}}\sqrt{\left(\dfrac{\mu_{mn}}{R}\right)^2+\left(\dfrac{p\pi}{\Delta h}\right)^2} & TM_{mnp}\end{cases}, \quad (1)$$

where μ_r and ε_r are relative permeability and permittivity of the filling material, respectively, μ_{mn} and μ'_{mn} are the n^{th} roots of the m^{th} Bessel function of the first kind and its derivative. The symbol R is the radius of the circular cavity, Δh is the height of the circular cavity, and c is the speed of light in free space. For $m > 0$, each m represents a pair of degenerate *TM* and *TE* modes (cos ($m\varphi$) or sin ($m\varphi$) variation). In circular cavity, TM_{110}, the second order mode, is selected as the working mode. Different directions represent different TM_{110} modes (cos ($m\varphi$) and sin ($m\varphi$) variation). μ_{mn} is 3.832 for the TM_{110} mode. Therefore, the corresponding resonant frequency of TM_{110} mode is,

$$f_{110}=\frac{c}{2\pi\sqrt{\mu_r\varepsilon_r}}\cdot\frac{3.832}{R}=\frac{0.61c}{R\sqrt{\mu_r\varepsilon_r}}. \quad (2)$$

Then, the radius of the SICC can be obtained by,

$$R=\frac{0.61c}{f_{110}\sqrt{\mu_r\varepsilon_r}}. \quad (3)$$

However, in an SIEC, the two *TM* modes are not degenerated and have different resonant frequencies. They are denoted by TM_{cmnp} and TM_{smnp} modes, respectively. The resonant frequency for elliptic cavity with solid wall can be calculated using [6, 7],

$$f_{mnp}=\frac{c\cdot\sqrt{q_{mnp}}}{R_a\pi e\sqrt{\mu_r\varepsilon_r}}=\frac{c}{\pi\sqrt{\mu_r\varepsilon_r}}\cdot\frac{\sqrt{q_{mnp}}}{\sqrt{R_a^2-R_b^2}} \quad (4)$$

$$\begin{aligned}&\text{Ce}_m(\xi_o, q)= 0, && \text{for } TM_{cm} \text{ mode}\\ &\text{Se}_m(\xi_o, q) = 0, && \text{for } TM_{sm} \text{ mode}\\ &\text{Ce}_m'(\xi_o, q)=0, && \text{for } TE_{cm} \text{ mode}\\ &\text{Se}_m'(\xi_o, q)=0, && \text{for } TE_{sm} \text{ mode},\end{aligned} \quad (5)$$

where R_a and e are the semi-major axis and ellipticity of the SIEC, $\cosh(\xi_o) = 1 / e$. R_b is the semi-minor axis. The parameter q is related to the resonant frequency, and there are a series of q values satisfying equation (5). To avoid ambiguity, a third subscript n, corresponding to the n^{th} parametric root, is required in the mode designation, q_{mnp} is the n^{th} parametric zero of the modified Mathieu functions of the first kind of the order m or their derivatives. Because of Mathieu functions' complicated calculation process, it is not very convenient to compute the parameters of a dual mode SIEC from equation (4). Accordingly, the corresponding resonant frequency of quasi TM_{110} also can be computed by following approximate formula,

$$f_{c110}=\frac{c}{2\pi\sqrt{\mu_r\varepsilon_r}}\cdot\frac{1}{R_a}\cdot\sqrt{\frac{120(2e^4-15e^2+28)}{17e^4-114e^2+198}}. \quad (6)$$

The resonant frequencies between the simulated results and the one obtained from equation (6) are compared as illustrated in Table 1. Since of a good agreement between the simulated and calculated results, it is concluded that the approximate formula can be used to determine the initial parameters of a dual-mode SIEC. Next, the solid wall is replaced by metallic vias to form SICC and SIEC under the guideline of [4, 5, 14]. The resonant frequencies of $TM_{\text{c}110}$ and $TM_{\text{s}110}$ modes are approximately equal for the smaller ellipticity e. Consequently, using equations (3) and (6) the initial dimensions of the cavities are determined for a desired resonant frequency.

Figure 2 shows the electrical fields of the TM_{110} and quasi TM_{110} modes within the SICC and SIEC, respectively. Obviously, they are two orthogonal modes, which co-exist in the same cavity. The fields of the modes are distributed in different directions (cos (φ) or sin (φ) variation). The two degenerate modes in the SICC can be easily excited by setting the angle α between 100 and 130 degrees. Besides, the $TM_{\text{c}110}$ and $TM_{\text{s}110}$ modes within the SIEC contribute to TZs located at lower sideband and are engaged in passband forming.

C. Coupling slot

As shown in Fig. 3, two poles and four TZs are found in the response of a dual-mode complementary filter. Two poles below the zero Z_{1up} are denoted as P_1 and P_2, respectively. The first and second zeros near the passband are denoted as Z_{1d} and Z_{1up}, respectively. Being so close to the passband, zeros Z_{1d} and Z_{1up} are both helpful to realize a steeper side response. The coupling slot size determines the position of the first zero and then sets the slope of the side response. Figures 4 and 5 illustrate variations of poles, zeros as the coupling slot sizes changed. The distance between the zero Z_{1d} and pole P_1 is decreased as the coupling slot size W_{S} or θ increased, but the frequency of P_1,

Z_{2up} is decreased evidently. Meanwhile, a change occurs in the frequency of P_2 and Z_{1up}.

Table 1: Resonance frequencies obtained from the simulation and equation (6).

	R_a, R_b (mm)	Simulation (GHz)	Calculated (GHz)	Error (%)
1	6, 5.21	22.101	22.216	+0.52
2	8, 6.96	15.513	15.475	-0.25
3	10, 8.045	13.485	13.362	-0.91
4	12, 9.756	11.156	11.131	-0.23
5	13.4, 10.6	9.936	9.976	+0.40
6	16, 12.87	8.366	8.351	-0.18

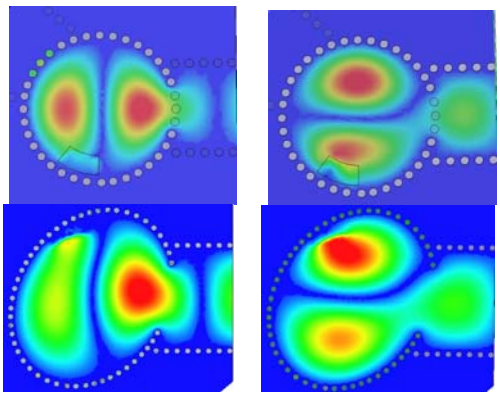

(a) Vertical mode (b) Horizontal mode

Fig. 2. The E-field distributions of the degenerate TM_{110} and quasi TM_{110} modes in SICC and SIEC.

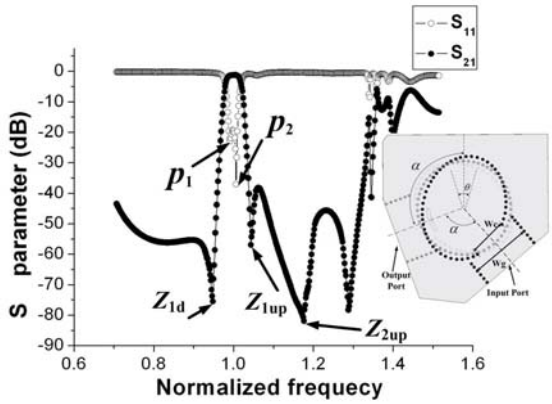

Fig. 3. Response of dual-mode complementary filter with SICC and SIEC.

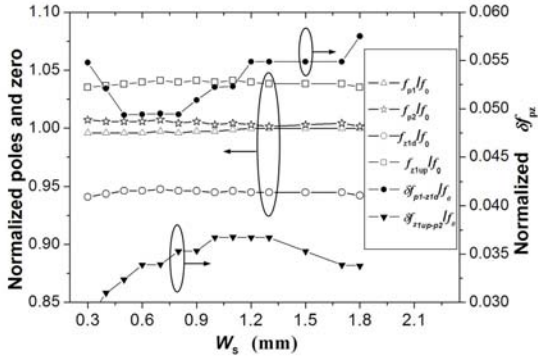

Fig. 4. Variation of poles, zeros with W_S, where, $\delta f_{p1\text{-}z1d} = f_{p1} - f_{p2}$, $\delta f_{z1up\text{-}P2} = f_{z1up} - f_{p2}$, $\theta = 36^o$, f_0 is the Eigen frequency of TM_{110} mode.

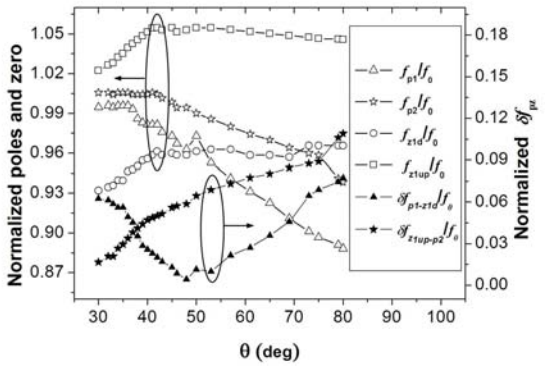

Fig. 5. Variation of poles, zeros with θ, where, Ws = 0.6 mm, $\delta f_{p1\text{-}z1d} = f_{p1} - f_{p2}$, $\delta f_{z1up\text{-}P2} = f_{z1up} - f_{p2}$.

As shown in Table 2, the coupling is increased when the slot size is increased. Then, it is possible to control the bandwidth and the rejection level. When the slot size is changed, the positions of P_1, P_2, Z_{1d}, and Z_{1up} influence the operating frequency. As observed in Figs. 4 and 5, the distance between the zero Z_{1d} and pole P_1 decreases evidently with the width of coupling slots W_S or θ decreases.

As observed in Table 3, the angle α also affects the bandwidth of the filter. A large value of α should be chosen for a broadband filter, while a small α may be proper for a narrowband filter. The proper value of α is between 100 and 130 degrees. Besides, the ellipticity e determines the position of the first zero Z_{1d}. As illustrated in Table 4, the ellipticity e is also an important factor affecting the bandwidth. So, a large value of e should be chosen for a broadband filter and vice versa.

Table 2: Relative bandwidth change with θ and W_s.

θ(deg)	$\Delta f/f_0$ (%)	W_s(*mm*)	$\Delta f/f_0$ (%)
30	3.3	0.3	3.10
35	3.6	0.4	3.50
38	4.1	0.6	3.95
40	4.39	0.7	4.10
60	4.5	0.8	4.15

Table 3: $\Delta f/f_0$ change with α.

W_c/R	α (deg)	$\Delta f/f_0$ (%)
0.785	110	3.9
0.785	120	4.1
0.785	130	4.2

Table 4: Relative bandwidth change with *e*.

e	W_c/R	α (deg)	$\Delta f/f_0$ (%)
0.569	0.81	110	2.77
0.587	0.81	110	3.61
0.592	0.81	110	3.85
0.612	0.81	110	4.06
0.646	0.81	110	4.20

D. External feeding structure

The filter is excited by a tapered microstrip lines. Energy travels from the microstrip line into the SIEC resonators and then is magnetically coupled into the adjacent SICC by means of coupling slots.

Moreover, the bandwidth and rolloff slope in the transition band are affected by W_c/R for a given angle α, as shown in Table 5. In general, smaller W_c/R leads to narrower bandwidth and steeper rolloff slope in the transition band.

Table 5: $\Delta f/f_0$ change with W_c/R.

W_c/R	α (deg)	$\Delta f/f_0$ (%)	W_c/R	α (deg)	$\Delta f/f_0$ (%)
0.72	110	3.60	0.79	130	4.3
0.78	110	3.87	0.88	130	4.5
0.87	110	4.10	0.96	130	4.8

E. Design consideration

As shown in Fig. 6, a SICC and SIEC techniques can be employed together to achieve multilayer filter. Nevertheless, its selectivity is lower, and absence of geometric symmetry makes more difficulties in adjustment. So, to achieve higher selectivity, symmetrical structures are proposed as the input/output ports, i.e., double SIECs combined with a SICC.

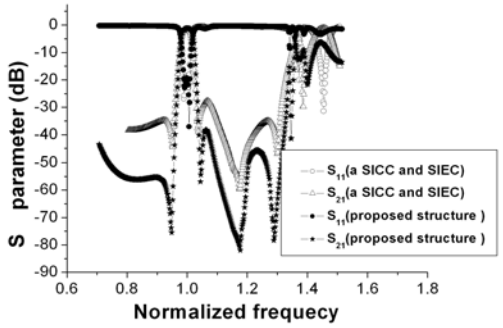

Fig. 6. Responses of multilayer dual-mode filters.

F. Design example

In our design, the center frequency and bandwidth of the filter are 10 GHz and 400 MHz, respectively. The used substrate is Rogers 5880 with relative permittivity (ε_r) of 2.2 and height of 0.508 mm. Here, the SICC and SIEC operate at TM_{110} and quasi TM_{110} modes, respectively. In the present design, the first step is to decide the dimensions of SICC and SIEC cavities. By using equations (2) and (3), the initial values of radius of SICC cavities (R) should be 12.3 mm. According to equation (6) and Table 4, the semi-major (R_a) and semi-minor (R_b) axes of the SIEC should be 13.3 mm and 10.7 mm, respectively.

The second step is to calculate the coupling coefficients and external quality factor. The coupling scheme of the proposed dual-mode complementary filter is presented in Fig. 7. Resonators 1, 2 and resonators 3, 4 represent two orthogonal modes, respectively. From the above discussion, the initial geometrical parameters of slot and cavities will be determined as follow:

i) Based on the above discussion, the angle α is the key factor to realize the dual-mode character in multilayer SICCs and SIECs. As shown in Fig.1, the angle between the coupling slot 1 and input port is set to α in order to realize dual-mode in cavity 1. And then, the angle between the coupling slots 1 and 2 is also equal to α so that degenerate modes can exist in cavity 2. Similarly, the angle between the coupling slot 2 and output port must be kept as α in cavity 3. Based on the specification, the proper value of α is 110°.

ii) The coupling slot size determines the bandwidth and the positions of the zeros. According to Figs. 4, 5 and Table 2, the initial geometrical parameters of the slot are determined. One can choose the width of the coupling slot with $W_S = 0.6$ mm, the central angle $\theta = 38^o$.

iii) The bandwidth and rolloff slope in the transition band are affected by W_c/R. As shown in Table 5, the widths of the coupling apertures are determined as $W_c/R = 0.8$. For a given angle $\alpha = 110^o$, the proper parameters are limited in a relatively narrow interval. According to Table 5 and the specifications, the value ranges for W_c/R are from 0.75 to 0.85. Similarly, as observed in Table 2, the value ranges for W_S, θ are from 0.6 to 0.8 and from 35^o to 39^o, respectively. According to the above considerations, the final optimal dimensions of the proposed filter can be easily determined.

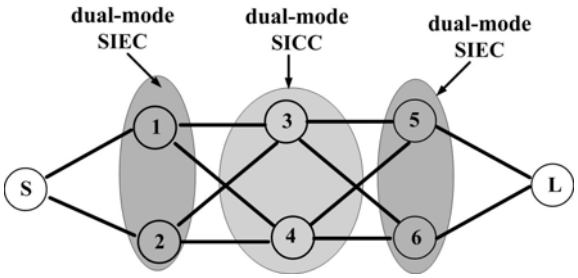

Fig. 7. Coupling scheme of the sixth-order dual-mode filter (gray areas show dual-mode cavities).

III. EXPERIMENT RESULTS

Based on the above-discussed theories, the multilayer dual-mode complementary filter is designed and fabricated with PCB process. Figure 8 is the photograph of the fabricated dual-mode filter. After optimization being implemented by Ansoft HFSS, the geometry parameters of the proposed filter are listed in Table 6. The metallic via diameter is 0.8 mm. The space between two adjacent vias is uniformly arranged around 1.5 mm.

Table 6: Parameters of the fabricated filter.

Dvia(mm)	0.8	Wstrip(mm)	1.58
p(mm)	1.5	Wg (mm)	16
ε_r	2.2	Wc (mm)	10.5
Ws(mm)	0.7	h(mm)	0.508
α(deg)	110	R(mm)	12.2
θ(deg)	37	R_a(mm)	13.6
R_b(mm)	10.7		

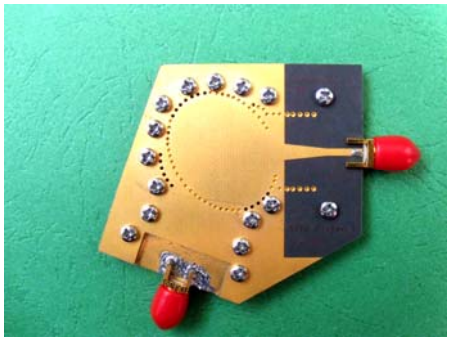

Fig. 8. Photograph of the fabricated filter.

As observed from Fig. 9, the fabricated filter has a center frequency of 9.95 GHz with a bandwidth of 397.6 MHz. The maximum return loss of the proposed filter is 19.5 dB and the insertion loss is about 2.35 dB. Three finite transmission zeros are located at 9.4, 10.3, and 11 GHz, respectively. Its stop band is from 7.8 GHz to 9.45 GHz with the rejection more than 50 dB, and from 10.8 GHz to 12.9 GHz with the rejection more than 45 dB. Table 7 gives some reported performance of SIW filters in recent years for comparison purposes and it demonstrates that this work has realized miniaturization and improved selectivity.

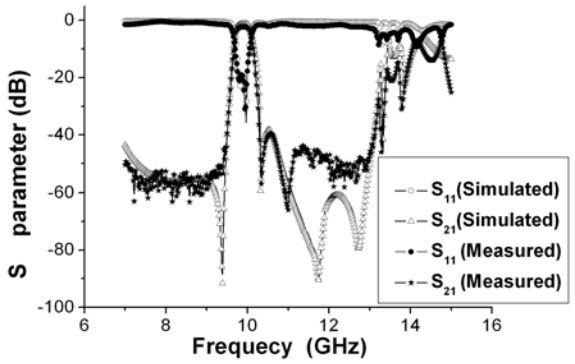

Fig. 9. Simulated and measured results of the dual-mode complementary filter with three layers.

IV. CONCLUSION

A novel multilayer dual-mode complementary filter has been designed, fabricated, and measured in this paper. The complementary SICC and SIEC are introduced in the 3-D multilayer SIW circuits, and a compact dual-mode filter with low loss and elliptic response has been achieved. The bandwidth and restraint outside the band can be

controlled by adjusting the parameters of the coupling aperture and arc-shaped slot. The measured maximum return loss is 19.5 dB over the passband while the insertion loss is about 2.35 dB. In particular, measured results show that the stopband rejection of the filter is better than 50 dB. Good agreement is obtained between the simulated and measured results of the proposed structure. This structure is very compact and well suited for the microwave and millimeter wave applications.

Table 7: Performance comparison of the SIW filters.

Ref.	Size (λ_g^2)/ Number of layers and TZs	f_0 (GHz)	Stopband rejection / IL(dB)
[4]	6.80/1/1	14.60	30/3.5
[5]	4.80/2/2	20	16/2.2
[8]	6.36/1/1	25.53	30/2.5
[9]	5.29/4/2	30	25/2.95
This work	4.10/3/4	9.95	50/2.35
Where λ_g is the guided wavelength on the substrate at the center frequency f_0.			

ACKNOWLEDGMENT

This work is supported in part by the National Natural Science Foundation of China (NSFC) under grant 61001028 and in part by Research Fund for the Doctoral Program of Higher Education of China (RFDP) under grant 2010018511001，and in part by the Fundamental Research Funds for the Central Universities under grant ZYGX2010J019.

REFERENCES

[1] X. P. Chen and K. Wu, "Substrate integrated waveguide filter with improved stopband performance for satellite ground terminal," *IEEE Trans. Microw. Theory Tech.*, vol. 57, no. 3, pp. 674-683, March 2009.

[2] W. Shen, W. Y. Yin, and X. W. Sun, "Compact substrate integrated waveguide (SIW) filter with defected ground structure," *IEEE Microw. Wirel. Compon. Lett.*, vol. 21, no. 2, pp. 83-85, Feb. 2011.

[3] D. Deslandes and K. Wu, "Substrate integrated waveguide dual-mode filters for broadband wireless systems," *RAWCON '03. Proceedings*, pp. 385-388, Aug. 2003.

[4] B. Potelon, J. F. Favennec, E. Rius, and J. C. Bohorquez, "Design of a substrate integrated waveguide (SIW) filter using a novel topology of coupling," *IEEE Microw. Wirel. Compon. Lett.*, vol. 18, no. 9, pp.596-598, Sep. 2008.

[5] Q. -F. Wei, Z. -F. Li, and L. -S. Wu, "Compact cross-coupled circular cavity filters using multilayer substrate integrated waveguide," *Electron. Lett.* vol. 45, no. 6, 12th March 2009.

[6] S. J. Zhang and Y. C. Shen, "Eigenmode sequence for an elliptical waveguide with arbitrary ellipticity," *IEEE Trans. Microw. Theory Tech.*, vol. 43, no. 1, pp. 227-230, Jan. 1995.

[7] L. Accatino, G. Bertin, and M. Mongiardo, "Elliptical cavity resonators for dual-mode narrow-band filters," *IEEE Trans. Microw. Theory Tech.*, vol. 45, no. 12, pp. 2393-2401, Dec. 1997.

[8] H. J. Tang, W. Hong, J. -X. Chen, G. -Q. Luo, and K. Wu, "Development of millimeter-wave planar diplexers based on complementary characters of dual-mode substrate integrated waveguide filters with circular and elliptic cavities," *IEEE Trans. Microw. Theory Tech.*, vol. 55, no. 4, pp.776-781, April 2007.

[9] K. Ahn and I. Yom, "A ka-band multilayer LTCC 4-pole bandpass filter using dual-mode cavity resonators," *Microwave Symposium Digest*, *2008 IEEE MTT-S International*, pp.1235-1238, June 2008.

[10] R. Rezaiesarlak, M. Salehi, and E. Mehrshahi, "Hybrid of moment method and mode matching technique for full-wave analysis of SIW circuits," *Appl. Comp. Electro. Society (ACES) Journal*, vol. 26, no. 8, pp. 688-695, August 2011.

[11] W. Shao and J. L. Li, "Design of a half-mode SIW high-pass filter," *Appl. Comp. Electro. Society (ACES) Journal*, vol. 26, no. 5, pp. 447-451, May 2011.

[12] R. Q. Li, X. H. Tang, and F. Xiao, "Substrate integrated waveguide dual-mode filter using slot lines perturbation," *Electron. Lett.*, vol. 46, no. 12, 10th June 2010.

[13] D. M. Pozar, *Microwave Engineering,* 2nd Edition, Wiley, New York, 1998.

[14] F. Xu and K. Wu, "Guided-wave and leakage characteristics of substrate integrated waveguide," *IEEE Microw. Theory Tech.*, vol. 53, no. 1, pp. 66-70, Jan. 2005.

Zhigang Zhang was born in Shanxi Province, China. He received the B.Sc. degree in Electronic Information Engineering and M.Sc. degree in wireless physics from Sichuan University and is currently working toward the Ph.D. degree in electromagnetic field and microwave technology from The University of Electronic Science and Technology of China (UESTC), Chengdu, Sichuan, China. His current research interests include SIW technology and its application, microwave and millimeter-wave filters and couplers, electromagnetic theory.

Yong Fan received the B.E. degree from the Nanjing University of Science and Technology, Nanjing, Jiangsu, China, in 1985, and the M.Sc. degree from the University of Electronic Science and Technology of China (UESTC), Chengdu, Sichuan, China, in 1992. He is currently with the School of Electronic Engineering, UESTC. He has authored or coauthored over 60 papers. From 1985 to 1989, he was interested in microwave integrated circuits. Since 1989, his research interests include millimeter-wave communication, electromagnetic theory, millimeter-wave technology, and millimeter-wave systems. Mr. Fan is a Senior Member of the Chinese Institute of Electronics (CIE).

Yonghong Zhang received the B.Sc., M.Sc., and Ph.D. degrees from the University of Electronic Science and Technology of China (UESTC), Chengdu, China, in 1992, 1995, and 2001, respectively. From 1995 to 2002, he was a Teacher with the UESTC. In 2002, he joined the Electronic Engineering Department, Tsinghua University, Beijing, China, as a Doctoral Fellow. In 2004, he rejoined the UESTC. His research interests are in the area of microwave and millimeter-wave technology and applications.